

Machine Learning-Based CSI Feedback With Variable Length in FDD Massive MIMO

Matteo Nerini, Valentina Rizzello, *Student Member, IEEE*, Michael Joham, *Member, IEEE*, Wolfgang Utschick, *Fellow, IEEE*, Bruno Clerckx, *Fellow, IEEE*

Abstract—To fully unlock the benefits of multiple-input multiple-output (MIMO) networks, downlink channel state information (CSI) is required at the base station (BS). In frequency division duplex (FDD) systems, the CSI is acquired through a feedback signal from the user equipment (UE). However, this may lead to an important overhead in FDD massive MIMO systems. Focusing on these systems, in this study, we propose a novel strategy to design the CSI feedback. Our strategy allows to optimally design variable length feedback, that is promising compared to fixed feedback since users experience channel matrices differently sparse. Specifically, principal component analysis (PCA) is used to compress the channel into a latent space with adaptive dimensionality. To quantize this compressed channel, the feedback bits are smartly allocated to the latent space dimensions by minimizing the normalized mean squared error (NMSE) distortion. Finally, the quantization codebook is determined with k -means clustering. Numerical simulations show that our strategy improves the zero-forcing beamforming sum rate by 17%, compared to CsiNetPro. The number of model parameters is reduced by 23.4 times, thus causing a significantly smaller offloading overhead. At the same time, PCA is characterized by a lightweight unsupervised training, requiring eight times fewer training samples than CsiNetPro.

Index Terms—CSI feedback, frequency division duplex, k -means clustering, machine learning, massive MIMO, principal component analysis.

I. INTRODUCTION

ACCURATE knowledge of the wireless channel, or channel state information (CSI), is critical to unlock the full potential benefits of multiple-input multiple-output (MIMO) systems. In particular, CSI at the transmitter and at the receiver allow precoding and combining techniques, respectively, which can enhance the spectrum efficiency in MIMO wireless networks [1]. CSI at the transmitter can be easily acquired without feedback from the receiver in time division duplex (TDD) systems. In these systems, channel reciprocity holds since the uplink and downlink channels share the same frequency band. Conversely, CSI estimation at the transmitter is harder in frequency division duplex (FDD) systems, where the uplink-downlink channel reciprocity does not hold in general. Thus, feedback messages from the user equipment (UE) to the base station (BS) are needed to gain downlink

CSI at the BS [2]. This may lead to significant overhead in massive MIMO systems, where a large number of antennas is employed. To face this problem, various strategies have been investigated, such as downlink training techniques [3], distributed compressive CSI estimation for multi-user settings [4], and adaptive CSI feedback depending on the channel sparsity [5]. Additionally, novel transmission strategies robust with respect to reduced-dimensional CSI have been proposed [6]–[8].

In recent years, deep learning (DL) techniques have been also used for CSI estimation in FDD systems, following two main research directions. In the first, the uplink-to-downlink channel mapping is learned. In this way, the feedback can be completely removed since the uplink channel knowledge at the BS is sufficient to gain also the downlink channel knowledge. In the second, the channel matrix is compressed with a DL architecture to minimize the feedback.

The uplink-to-downlink mapping existence was firstly investigated in [9]. In [9], [10], a fully connected neural network (NN) is used to map the uplink to the corresponding downlink channels. The same task is solved more efficiently in [11] with a sparse complex-valued NN, and in [12], [13] with a convolutional neural network (CNN) treating the space-frequency channel matrix as an image. Image processing techniques are exploited also in [14], [15]. Finally, in [16], the channel is firstly compressed with an autoencoder to decrease the feature space dimensionality; then, the uplink-to-downlink mapping is achieved with random forests. However, when more complex channel models are considered (e.g. accounting for a rich multipath and dynamic environment), the uplink-to-downlink mapping function becomes hard to approximate with NNs. The environment should be sampled with enough resolution to account for small-scale fading effects, which may require extensive sampling campaigns and huge datasets in practice. For this reason, the vast majority of related studies used DL techniques to reduce the feedback overhead, rather than completely remove it.

In [17], [18], a deep autoencoder is used to embed the downlink channel matrix at the UE into a latent space with reduced dimensionality. In this way, only the embedding of the channel matrix needs to be fed back to the BS. Deep autoencoder-like architectures have been proposed for the same scope in [19]–[25]. The CsiNet architecture introduced in [19] is extended in [26] to exploit the temporal redundancy in a dynamic environment through recurrent layers, and further

M. Nerini and B. Clerckx are with the Department of Electrical and Electronic Engineering, Imperial College London, London, SW7 2AZ, U.K. (e-mail: {m.nerini20, b.clerckx}@imperial.ac.uk).

V. Rizzello, M. Joham and W. Utschick are with the Professur für Methoden der Signalverarbeitung, Technische Universität München, Munich, 80333, Germany. (e-mail: {valentina.rizzello, joham, utschick}@tum.de).

Manuscript received April 11, 2022; revised August 08, 2022.

improved in [27], [28]. In [20], the channel reconstruction accuracy is enhanced by exploiting also information from the uplink CSI, assumed available at the BS. In [21], [22], a DL-based framework is proposed to jointly learn CSI compression and quantization. In [23]–[25], the CSI feedback is designed through lightweight DL architectures, characterized by a reduced number of trainable parameters. To improve the compression performance and reduce the model complexity, the novel concepts of network aggregation and layer binarization have been employed in [29]. Furthermore, the low rank structure of the millimeter wave channels has been exploited by the model-driven DL architecture proposed in [30].

Other related works employ DL techniques either at the BS or at the UE to improve the channel reconstruction quality or the feedback design, respectively. In [31], [32], the feedback is generated at the UE by sampling only specific entries of the downlink channel matrix. Then, the original channel matrix is reconstructed at the BS with image-restoration CNNs. Similarly, in [33], the channel is compressed at the UE based on compressive sensing and then recovered through a DL architecture at the BS. In [34], a NN has been proposed to directly map noisy pilot observations to their optimal feedback index. In [35], NNs are used to design an implicit CSI feedback mechanism in which the CSI is mapped into the recommended precoder. Finally, DL architectures have been applied to learn feedback messages with the objective of maximizing the downlink precoding performance in single-cell [36], and multi-cell [37] scenarios.

When applying DL models for designing the CSI feedback, three problems arise. First, very large training datasets are typically required: e.g., hundreds of thousands of downlink training samples are used in many of the aforementioned studies [9], [11], [16], [17], [19], [24], [27], [29], [33], [35], [37]. This problem has been recently addressed by training the DL architectures solely with uplink channel samples, assumed available at the BS [18], [32], [34], [38], [39]. These works exploit the conjecture that learning at the uplink frequency can be transferred at the downlink frequency with no further modification, as proposed for the first time in [32] and validated in [38]. Furthermore, this problem has been addressed through transfer learning in [40]. Second, to optimally generate variable length quantized feedback in massive MIMO systems, three problems need to be solved: *i*) CSI compression into a latent space with dimensionality depending on the number of feedback bits, *ii*) allocation of feedback bits to the latent space dimensions, and *iii*) design of the quantization levels. However, autoencoders compress the CSI into a latent space with fixed dimensionality, determined by the number of neurons present in their middle layer. As a result, the latent space dimensionality cannot be adapted to the number of feedback bits, leading to performance degradation in two cases. On the one hand, the performance significantly degrades when the number of feedback bits is too low compared to the latent space dimensionality, and it is not sufficient to properly quantize the too large latent space. On the other hand, when a high number of feedback bits is considered, the performance does not improve beyond the upper bound caused by the fixed latent space dimensionality. Two solutions to this problem are provided in [27], [33], where the authors

propose a DL-based method offering multiple compression ratios. However, the number of available compression ratios is still limited to four in [27], and the problem of optimally allocating the feedback bits to the compressed CSI dimensions is not investigated in neither study. The problem of allocating the bits to the compressed CSI dimensions is relevant since they may carry different amount of information. Nevertheless, this problem remains unexplored in recent literature proposing DL solutions. Third, each UE must encode the CSI by using the DL architecture trained at the BS. Thus, the trained architecture parameters need to be offloaded from the BS to the UE when a new UE connects to the BS, and after each training session. This causes an additional fixed overhead in the transmission, which cannot be reduced.

To solve these three problems affecting DL models, we propose an alternative approach avoiding the use of DL. Differently from previous literature, we compress the CSI with principal component analysis (PCA), a classical machine learning (ML) technique [41]. PCA offers a useful property that cannot be found in typical DL architectures used for compression: the latent space dimensions explain different variances and can be ordered according to their importance. This property allows us to introduce a novel and practical bit allocation technique that assigns the available feedback bits to the latent space dimensions. Coupling PCA with our novel bit allocation, we show that our technique performs better, or approximately equal, than DL architectures recently proposed for the same scope. Besides the channel reconstruction quality improvement, our approach brings three fundamental benefits compared to related works using DL solutions. First, it is characterized by a lightweight training phase not involving costly iterative optimization algorithms and requiring a reduced number of training samples. Second, our technique adapts the latent space dimensionality to the number of feedback bits. Thus, variable length feedbacks can be optimally generated with a unique trained model. Third, our technique can be implemented with a variable number of model parameters. This enables the network operator to trade the reconstruction quality and the communication overhead due to the model parameter offloading in an adaptive manner. These benefits allow our approach to efficiently design variable length CSI feedback, whose advantages are promising compared to fixed feedback [5], [42]. It has been shown that the CSI reconstruction can be greatly improved by adjusting the feedback overhead according to the sparsity level of the channels [5]. Also in a multi-user setting, the sum rate improves when the total feedback bits are smartly distributed among the users, employing a feedback with adaptive length [42]. The contributions of this paper are summarized as follows.

First, we propose a novel CSI feedback strategy based on PCA and k -means clustering. In this strategy, PCA is used to compress the channel matrix into a latent space with adaptive dimensionality, allowing to optimally design the feedback with variable length. To quantize this compressed channel, the feedback bits are smartly allocated to the principal components in order to minimize a properly defined distortion function. Finally, on each principal component, the quantization levels are determined with vector quantization. Specifically, we em-

ploy k -means clustering since it is the fixed-rate quantization strategy that minimizes the mean squared error (MSE) by construction.

Second, we provide theoretical justifications to prove the optimality of our bit allocation to the principal components. In our approach, the bits are allocated to the principal components by minimizing the normalized mean squared error (NMSE) distortion introduced by the compression and quantization operations. Despite optimal bit allocation is a popular concept in wireless communications [42], the optimal feedback bits allocation to the CSI principal components has never been investigated before. A practical iterative algorithm is proposed to this scope, whose optimality is theoretically guaranteed.

Third, we propose an offloading overhead-aware CSI feedback by improving our PCA-based strategy with two modifications. The first reduces the number of offloaded PCA parameters, while the second reduces the number of offloaded codebook parameters. With these two modifications, the number of offloaded parameters can be adapted. Thus, the network operator can select the optimal trade-off between offloading overhead and CSI reconstruction quality. To the best of our knowledge, an adaptive offloading overhead has never been considered in previous literature employing DL solutions. Results show that these two modifications only slightly impact the reconstruction performance, while they significantly reduce the number of offloaded parameters.

Fourth, we compare the performance of our strategy with two state-of-the-art DL autoencoders proposed for the same scope. As a benchmark, we consider CsiNetPro [28], the improved version of the popular CsiNet [19], and the autoencoder more recently proposed in [18] whose training is based on uplink data. Our strategy is characterized by a lightweight training phase, requiring significantly fewer training samples. The number of offloaded model parameters can be reduced with approximately no CSI reconstruction quality loss. Consequently, our strategy causes less offloading overhead than the considered reference autoencoders. At the same time, our strategy achieves better or approximately the same CSI reconstruction quality as these autoencoders.

Organization: In Section II, we define the system model and the problem formulation. In Section III, we present our novel CSI feedback strategy based on PCA and k -means clustering. In Section IV, we improve our CSI feedback strategy by proposing two modifications that allow to significantly decrease the number of offloaded parameters. In Section V, we assess the obtained performance through numerical simulations. Finally, Section VI contains the concluding remarks. For reproducible research, the simulation code is available at <https://github.com/matteonerini/ml-based-csi-feedback>.

Notation: Vectors and matrices are denoted with bold lower and bold upper letters, respectively. Scalars are represented with letters not in bold font. $|a|$, $\|\mathbf{a}\|$, and $\|\mathbf{A}\|_F$ refer to the absolute value of a complex scalar a , l_2 -norm of a vector \mathbf{a} , and Frobenius norm of a matrix \mathbf{A} , respectively. $[\mathbf{a}]_i$ denotes the i -th element of vector \mathbf{a} . \mathbf{A}^T and \mathbf{A}^H refer to the transpose and conjugate transpose of a matrix \mathbf{A} , respectively. \mathbb{N} , \mathbb{R} , and \mathbb{C} denote natural, real, and complex number sets, respectively. \mathbb{N}^* denotes the positive natural number set. $\mathbf{0}$ and \mathbf{I} refer to an

all-zero matrix and an identity matrix, respectively. $\mathcal{CN}(0, \sigma^2)$ denotes the distribution of a circularly symmetric complex Gaussian (CSCG) random variable whose real and imaginary parts are independent normally distributed with mean zero and variance $\sigma^2/2$. $\mathcal{CN}(\mathbf{0}, \mathbf{R})$ denotes the distribution of a CSCG random vector with mean vector $\mathbf{0}$ and covariance matrix \mathbf{R} . Finally, $\text{diag}(a_1, \dots, a_N)$ refers to a diagonal matrix whose diagonal elements are a_1, \dots, a_N .

II. SYSTEM MODEL

Let us consider a multi-user MIMO system in which a BS equipped with N_A antennas serves K single-antenna users. Assuming an FDD communication system, we denote with f_{UL} and f_{DL} the uplink and downlink center frequencies, respectively. In both frequencies, the channel bandwidth W is divided into N_C orthogonal frequency division multiplexing (OFDM) subcarriers.

We denote as $x_{UL,q,n_C} \in \mathbb{C}$ the uplink signal transmitted by the q -th user on the n_C -th uplink subcarrier, and as $\mathbf{y}_{UL,n_C} \in \mathbb{C}^{N_A \times 1}$ the uplink signal received by the BS on the n_C -th uplink subcarrier. Thus, we have

$$\mathbf{y}_{UL,n_C} = \sum_{q=1}^K \mathbf{h}_{UL,q,n_C} x_{UL,q,n_C} + \mathbf{n}_{UL,n_C}, \quad (1)$$

where $\mathbf{h}_{UL,q,n_C} \in \mathbb{C}^{N_A \times 1}$ is the uplink channel vector seen by the q -th user on the n_C -th uplink subcarrier, and \mathbf{n}_{UL,n_C} is the additive white Gaussian noise (AWGN) at the n_C -th uplink subcarrier. Similarly, we denote as $\mathbf{x}_{DL,n_C} \in \mathbb{C}^{N_A \times 1}$ the downlink signal transmitted by the BS on the n_C -th downlink subcarrier, and as y_{DL,q,n_C} the downlink signal received by the q -th user on the n_C -th downlink subcarrier. Thus, we can write

$$y_{DL,q,n_C} = \mathbf{h}_{DL,q,n_C} \mathbf{x}_{DL,n_C} + n_{DL,q,n_C}, \quad (2)$$

where $\mathbf{h}_{DL,q,n_C} \in \mathbb{C}^{1 \times N_A}$ is the downlink channel vector seen by the q -th user on the n_C -th downlink subcarrier, and n_{DL,q,n_C} is the AWGN at the n_C -th downlink subcarrier.

Let us define $\mathbf{H}_{UL,q} = [\mathbf{h}_{UL,q,1}, \mathbf{h}_{UL,q,2}, \dots, \mathbf{h}_{UL,q,N_C}] \in \mathbb{C}^{N_A \times N_C}$ as the uplink channel matrix and $\mathbf{H}_{DL,q} = [\mathbf{h}_{DL,q,1}^T, \mathbf{h}_{DL,q,2}^T, \dots, \mathbf{h}_{DL,q,N_C}^T] \in \mathbb{C}^{N_A \times N_C}$ as the downlink channel matrix of the q -th user. For simplicity of notation, we drop the index q in the rest of the paper. We assume that noisy versions of the uplink channel matrices are available at the BS, denoted as

$$\tilde{\mathbf{H}}_{UL} = \mathbf{H}_{UL} + \mathbf{N}_{UL}, \quad (3)$$

where the entries of $\mathbf{N}_{UL} \in \mathbb{C}^{N_A \times N_C}$ are CSCG distributed such that $\mathbb{E}[\|\mathbf{H}_{UL}\|_F^2 / \|\mathbf{N}_{UL}\|_F^2] = SNR_{UL}$. Similarly, a noisy version of the downlink channel matrix is available at each UE, which is given by

$$\tilde{\mathbf{H}}_{DL} = \mathbf{H}_{DL} + \mathbf{N}_{DL}, \quad (4)$$

where $\mathbb{E}[\|\mathbf{H}_{DL}\|_F^2 / \|\mathbf{N}_{DL}\|_F^2] = SNR_{DL}$. In this system model, our goal is to reconstruct the downlink CSI \mathbf{H}_{DL} at the BS from limited feedback sent by the UE. To this end, we compress and quantize the CSI using two ML techniques: PCA and k -means clustering.

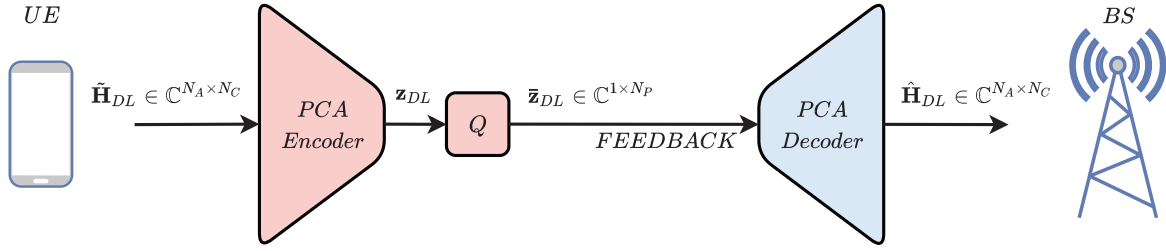


Fig. 1. Downlink channel estimation at the BS with quantized feedback from the UE.

III. PCA AND k -MEANS CLUSTERING-BASED CSI FEEDBACK DESIGN

In this section, we describe our novel channel estimation process, which consists of two stages. In the first stage, called *offline learning*, the compression strategy is learned at the BS, based on a reduced training dataset. This stage has three objectives: learning the principal components to compress the CSI, allocating the feedback bits to the first principal components, and learning the quantization levels through k -means clustering. In the second stage, called *online development*, the CSI is compressed and quantized at the UE, sent to the BS, and here reconstructed, as graphically represented in Fig. 1.

A. Offline Learning

To learn the principal components, we propose an offline training stage carried out at the BS. To this end, we consider a training set solely composed of noisy uplink channels, assumed available at the BS. This approach is based on the conjecture that learning at the uplink frequency can be transferred at the downlink frequency with no further modification [32], [38]. In this way, downlink CSI samples, which are hard to collect at the BS, are not required in the training stage. Let us denote with N_{train} the number of training samples, and with $\tilde{\mathbf{H}}_{\text{train}} \in \mathbb{C}^{N_{\text{train}} \times N_A N_C}$ the training set, whose rows are vectorized noisy uplink channels. Furthermore, we denote with $\boldsymbol{\mu}_{\text{train}}$ the column-wise mean of $\tilde{\mathbf{H}}_{\text{train}}$, and with $\mathbf{H}_{\text{train}}$ the centered training set obtained by subtracting $\boldsymbol{\mu}_{\text{train}}$ to each row of $\tilde{\mathbf{H}}_{\text{train}}$. Thus, the sample covariance matrix of the training set can be obtained as

$$\mathbf{R} = \frac{\mathbf{H}_{\text{train}}^H \mathbf{H}_{\text{train}}}{N_{\text{train}} - 1}. \quad (5)$$

With eigenvalue decomposition, \mathbf{R} can be factorized as $\mathbf{R} = \mathbf{V} \boldsymbol{\Lambda} \mathbf{V}^H$, where \mathbf{V} is a unitary matrix whose columns are the principal components, and $\boldsymbol{\Lambda} = \text{diag}(\sigma_1^2, \dots, \sigma_{N_A N_C}^2)$ is a diagonal matrix containing the $N_A N_C$ eigenvalues. Let us assume that the eigenvalues in $\boldsymbol{\Lambda}$ have been sorted in descending order, and that their respective eigenvectors in \mathbf{V} (i.e., the principal components) have been ordered accordingly. Thus, we can select the conversion matrix $\mathbf{V}_{N_P} \in \mathbb{C}^{N_A N_C \times N_P}$, containing the first N_P columns of \mathbf{V} , to project the data onto a latent space with dimensionality N_P .

After the dimensionality reduction operation, the compressed CSI needs to be discretized and represented with a limited number of bits B . According to a naive discretization

approach, we could fix the latent space dimensionality N_P arbitrarily, and quantize the compressed CSI by allocating B/N_P bits to each principal component. However, this approach would be suboptimal for two reasons. Firstly, N_P should be defined according to the number of feedback bits B . A higher B should allow a larger latent space dimensionality N_P , while, vice versa, a lower B should reduce N_P . Secondly, the N_P principal components have decreasing importance, defined as the variance explained by each of them. Thus, the optimal discretization approach is expected to allocate more bits to more important principal components, and fewer bits to the less important ones. To solve these two problems, we propose to allocate the B bits to the principal components in a way that minimizes the distortion introduced by the compression and quantization operations. As a result of this bit allocation process, the number of bits allocated to each principal component is described by the vector $\mathbf{b} = [b_1, \dots, b_{N_A N_C}] \in \mathbb{N}^{N_A N_C}$, where b_n is the number of bits allocated to the n -th principal component. Thus, we have $\sum_{n=1}^{N_A N_C} b_n = B$ and N_P is given by the index of the last non-zero element in \mathbf{b} . The proposed bit allocation process is described in detail in Subsection III-C.

After determining N_P and the bit allocation to the first N_P principal components, the quantization levels need to be specified. To minimize the quantization distortion, measured in terms of MSE, we define different quantization levels for each principal component, based on k -means clustering [41]. To this end, we project the training set $\mathbf{H}_{\text{train}}$ onto the first N_P principal components, obtaining $\mathbf{Z}_{\text{train}} = \mathbf{H}_{\text{train}} \mathbf{V}_{N_P} \in \mathbb{C}^{N_{\text{train}} \times N_P}$. In this way, the rows of $\mathbf{Z}_{\text{train}}$ are the embeddings of the training set elements into the latent space. Then, k -means clustering is applied independently to each column of $\mathbf{Z}_{\text{train}}$, where for the n -th column we have $k = 2^{b_n}$. Since each column of $\mathbf{Z}_{\text{train}}$ is a complex vector, each k -means clustering problem is considered as a vector quantization problem in the feature space \mathbb{R}^2 . In this problem, the two dimensions are given by the real and imaginary parts of the $\mathbf{Z}_{\text{train}}$ elements. Finally, the cluster centers of the n -th k -means clustering give the quantization levels for the n -th latent space dimension.

B. Online Development

After the *offline learning* stage, the first N_P principal components, the vector $\boldsymbol{\mu}_{\text{train}}$, and the codebook of the learned quantization levels are offloaded to the UE. This allows the online feedback process, as represented in Fig. 1. The UE firstly vectorizes the noisy downlink channel matrix $\tilde{\mathbf{H}}_{DL}$ into

$\tilde{\mathbf{h}}_{\text{DL}} \in \mathbb{C}^{1 \times N_A N_C}$. Then, it compresses $\mathbf{h}_{\text{DL}} = \tilde{\mathbf{h}}_{\text{DL}} - \boldsymbol{\mu}_{\text{train}}$ by considering only the first N_P principal components, obtaining $\mathbf{z}_{\text{DL}} = \mathbf{h}_{\text{DL}} \mathbf{V}_{N_P} \in \mathbb{C}^{1 \times N_P}$. Before the feedback transmission, the compressed CSI \mathbf{z}_{DL} is quantized according to the learned codebook. Therefore, $\bar{\mathbf{z}}_{\text{DL}}$ is obtained by mapping the \mathbf{z}_{DL} entries to their nearest cluster centers. In this way, the feedback is fully described by B bits, which are sent from the UE to the BS. Finally, the downlink channel estimation process is concluded at the BS. Here, the decoder firstly calculates $\hat{\mathbf{h}}_{\text{DL}} = \bar{\mathbf{z}}_{\text{DL}} \mathbf{V}_{N_P}^H \in \mathbb{C}^{1 \times N_A N_C}$; and secondly, it reshapes $\hat{\mathbf{h}}_{\text{DL}} + \boldsymbol{\mu}_{\text{train}}$ into $\hat{\mathbf{H}}_{\text{DL}}$, which is the downlink channel matrix estimate.

C. Bit Allocation to the Principal Components

Within the the *offline learning* stage, the optimal bit allocation to the principal components is learned. As anticipated, this is achieved by minimizing the distortion introduced by the compression and quantization operations. To measure such a distortion, we define a distortion function D_f given by the NMSE between the reconstructed vectorized channel $\hat{\mathbf{h}}_{\text{DL}}$ and the actual vectorized channel available at the UE \mathbf{h}_{DL}

$$D_f = \mathbb{E} \left[\frac{\|\mathbf{h}_{\text{DL}} - \hat{\mathbf{h}}_{\text{DL}}\|^2}{\|\mathbf{h}_{\text{DL}}\|^2} \right], \quad (6)$$

where the average is over all the channel realizations in the training set. Without loss of generality, we can write $\mathbf{h}_{\text{DL}} = \mathbf{g}_{\text{DL}} \mathbf{V}^H$, where $\mathbf{g}_{\text{DL}} = \mathbf{h}_{\text{DL}} \mathbf{V}$ is the mapping of \mathbf{h}_{DL} into the entire principal component space, and $\hat{\mathbf{h}}_{\text{DL}} = \bar{\mathbf{g}}_{\text{DL}} \mathbf{V}^H$, where $\bar{\mathbf{g}}_{\text{DL}}$ is the quantized version of \mathbf{g}_{DL} . Thus, the distortion function D_f can be rewritten as

$$D_f = \mathbb{E} \left[\frac{\|\mathbf{g}_{\text{DL}} \mathbf{V}^H - \bar{\mathbf{g}}_{\text{DL}} \mathbf{V}^H\|^2}{\|\mathbf{h}_{\text{DL}}\|^2} \right] \quad (7)$$

$$= \mathbb{E} \left[\frac{\|(\mathbf{g}_{\text{DL}} - \bar{\mathbf{g}}_{\text{DL}}) \mathbf{V}^H\|^2}{\|\mathbf{h}_{\text{DL}}\|^2} \right] \quad (8)$$

$$\leq \mathbb{E} \left[\frac{\|\mathbf{g}_{\text{DL}} - \bar{\mathbf{g}}_{\text{DL}}\|^2 \|\mathbf{V}^H\|_F^2}{\|\mathbf{h}_{\text{DL}}\|^2} \right] = \bar{D}_f, \quad (9)$$

where the inequality follows from the Cauchy-Schwarz inequality. We now assume that the training set has been normalized such that for every channel we have $\|\mathbf{h}_{\text{DL}}\|^2 = N_A N_C$. This has no impact on the multi-user precoding performance since the precoder design only requires the channel direction information (CDI). Thus, noting that $\|\mathbf{V}^H\|_F^2$ and $\|\mathbf{h}_{\text{DL}}\|^2$ are constant, the upper bound on the distortion function \bar{D}_f can be simplified as

$$\bar{D}_f = \mathbb{E} [\|\mathbf{g}_{\text{DL}} - \bar{\mathbf{g}}_{\text{DL}}\|^2] \quad (10)$$

$$= \mathbb{E} \left[\sum_{n=1}^{N_A N_C} |[\mathbf{g}_{\text{DL}}]_n - [\bar{\mathbf{g}}_{\text{DL}}]_n|^2 \right] \quad (11)$$

$$= \sum_{n=1}^{N_A N_C} \mathbb{E} [|[\mathbf{g}_{\text{DL}}]_n - [\bar{\mathbf{g}}_{\text{DL}}]_n|^2]. \quad (12)$$

We notice that the term $\mathbb{E} [|[\mathbf{g}_{\text{DL}}]_n - [\bar{\mathbf{g}}_{\text{DL}}]_n|^2]$ is the MSE due to the quantization of the n -th principal component. The MSE is a common metric used to measure the distortion

in lossy compression. Thus, to simplify the notation, we introduce the vector $\mathbf{d} = [d_1, \dots, d_{N_A N_C}]$, where $d_n = \mathbb{E} [|[\mathbf{g}_{\text{DL}}]_n - [\bar{\mathbf{g}}_{\text{DL}}]_n|^2]$. Consequently, our objective becomes to find the bit allocation \mathbf{b} such that $\bar{D}_f = \sum_{n=1}^{N_A N_C} d_n$ is minimized. Here, the implicit dependence of \bar{D}_f on \mathbf{b} lies in the fact that the distortion d_n depends on the number of bits b_n used to quantize the n -th principal component, and on the quantization strategy employed. Since the fixed-rate quantization strategy that minimizes d_n is k -means clustering, we consider d_n as the minimum distortion obtainable by k -means clustering with $k = 2^{b_n}$. In the following, we write $d_n = d_n(b_n)$ to highlight that d_n is a function purely dependent on b_n .

To design an algorithm able to find the optimal bit allocation \mathbf{b} , we now introduce two useful propositions. Let us assume that the channels are Rayleigh distributed, with covariance matrix \mathbf{R} . Thus, we have that the rows of $\mathbf{H}_{\text{train}}$ are distributed as $\mathcal{CN}(\mathbf{0}, \mathbf{R})$. Recalling that $\mathbf{R} = \mathbf{V} \boldsymbol{\Lambda} \mathbf{V}^H$, the rows of $\mathbf{G}_{\text{train}} = \mathbf{H}_{\text{train}} \mathbf{V}$ are distributed as $\mathcal{CN}(\mathbf{0}, \boldsymbol{\Lambda})$ [43]. In other words, since $\mathbf{G}_{\text{train}}$ is the training set projection onto the whole principal components space, we obtain that on every principal component the training set entries are CSCG distributed. More precisely, each entry of the n -th column of $\mathbf{G}_{\text{train}}$ is distributed as $\mathcal{CN}(0, \sigma_n^2)$, meaning that on the n -th principal component the training set entries are distributed as $\mathcal{CN}(0, \sigma_n^2)$. This property is used to derive the following two propositions.

Proposition 1. *If the optimal allocation of B bits is $\mathbf{b} = [b_1, \dots, b_{N_A N_C}]$, the optimal allocation of $B + 1$ bits is $\mathbf{b}' = [b_1, \dots, b_m + 1, \dots, b_{N_A N_C}]$ for some index $m \in [1, N_A N_C]$.*

Proof. Please refer to Appendix A. \square

In other words, the optimal allocation of $B + 1$ bits can be obtained from the optimal allocation of B bits by adding one bit to the m -th principal component, for some $m \in [1, N_A N_C]$. This allows us to recursively find the optimal bit allocation.

Proposition 2. *If the optimal allocation of B bits is $\mathbf{b} = [b_1, \dots, b_{N_A N_C}]$, we have $b_n \leq b_{n-1} \forall n \in [2, N_A N_C]$.*

Proof. Please refer to Appendix B. \square

Note that the \mathbf{b} elements are non increasing since the principal components are ordered according to their importance. This agrees with our intuition that more feedback bits should be allocated to more important principal components, and fewer bits to the less important ones.

We now use these two propositions to find the optimal bit allocation \mathbf{b} through Alg. 1. The objective of Alg. 1 is to return the bit allocation vector \mathbf{b} that minimizes the distortion function $\bar{D}_f = \sum_{n=1}^{N_A N_C} d_n$. To do so, we propose an iterative approach in which one bit at a time is added in \mathbf{b} , until all B bits are allocated, i.e., until $\sum_{n=1}^{N_A N_C} b_n = B$. Note that this iterative approach is able to lead to the optimal bit allocation because of Proposition 1. At the i -th iteration, the index of the \mathbf{b} element receiving the i -th bit could be found with exhaustive search. More precisely, for all the $N_A N_C$ principal components, the decrease in distortion caused by the additional bit could be computed and stored

Algorithm 1: Bit allocation to the principal components.

Input: $B, \mathbf{G}_{\text{train}}$
Output: \mathbf{b}

```

1  $\mathbf{b} \leftarrow [0, \dots, 0] \in \mathbb{N}^{N_A N_C}$ ;
2 for  $i \leftarrow 1$  to  $B$  do
3    $\Delta \mathbf{d} \leftarrow [0, \dots, 0] \in \mathbb{R}^{N_A N_C}$ ;
4   for  $n \leftarrow 1$  to  $N_A N_C$  do
5     if  $n == 1$  then
6        $\Delta d_n \leftarrow d_n(b_n) - d_n(b_n + 1)$ ;
7     else if  $b_n < b_{n-1}$  then
8        $\Delta d_n \leftarrow d_n(b_n) - d_n(b_n + 1)$ ;
9     end
10  end
11   $[\sim, m] \leftarrow \max(\Delta \mathbf{d})$ ;
12   $b_m \leftarrow b_m + 1$ ;
13 end
14 return  $\mathbf{b}$ 

```

in the vector $\Delta \mathbf{d} = [\Delta d_1, \dots, \Delta d_{N_A N_C}] \in \mathbb{R}^{N_A N_C}$, where $\Delta d_n = d_n(b_n) - d_n(b_n + 1)$. Consequently, the i -th bit could be allocated to the principal component experiencing the highest decrease in distortion (i.e., the m -th principal component in Alg. 1). However, this exhaustive search would require to explore $N_A N_C$ possibilities for the allocation of each bit. To significantly reduce the search space from $N_A N_C$ to only a few plausible principal components we resort to Proposition 2. If at the i -th iteration we have $b_n = b_{n-1}$, the n -th principal component will certainly not receive the i -th bit. Thus, the index n can be excluded from the search. As a consequence of Proposition 2, the number of plausible principal components that are eligible to receive the i -th bit becomes $b_1 + 1$ (i.e., a few units in practice).

The inputs of Alg. 1 are the number of feedback bits B , and the matrix $\mathbf{G}_{\text{train}}$, representing the projection of the training set $\mathbf{H}_{\text{train}}$ onto the whole principal components space. Here, $\mathbf{G}_{\text{train}}$ is needed to compute $d_n(b_n)$ through k -means clustering.¹ Furthermore, $d_n(0)$ is the maximum distortion for the n -th principal component, obtained by quantizing it with 0 bits. Thus, we have that $d_n(0)$ is the variance of the n -th column of $\mathbf{G}_{\text{train}}$, i.e., $d_n(0) = \sigma_n^2$. Finally, the output of Alg. 1 is the vector \mathbf{b} , whose n -th element represents the number of bits allocated to the n -th principal component. The latent space dimensionality N_P is returned implicitly as the index of the last non-zero element in \mathbf{b} . We remark that this bit allocation strategy is possible because of a specific property of PCA. In PCA, once the matrix \mathbf{V} is constructed upon a single training phase, all the latent space dimensionalities $N_P \in [1, \min\{N_{\text{train}} - 1, N_A N_C\}]$ can be considered for compression. Conversely, in autoencoders, this degree of freedom is not present since the latent space dimensionality is completely determined by the number of its

¹Note that if $N_{\text{train}} \leq N_A N_C$, only the first $N_{\text{train}} - 1$ columns of $\mathbf{G}_{\text{train}}$ are not null. Nevertheless, this does not affect our discussion if N_{train} is sufficiently large, i.e., $N_{\text{train}} > N_P$, where N_P is the last non-zero element in \mathbf{b} .

middle layer neurons.

D. Computational Complexity

The computational load required by our CSI feedback strategy is here assessed. Firstly, the complexity needed to obtain the sample covariance matrix \mathbf{R} and its eigenvalue decomposition is $\mathcal{O}(N_A^2 N_C^2 N_{\text{train}})$ and $\mathcal{O}(N_A^3 N_C^3)$, respectively. Secondly, the bits are allocated to the principal components through Alg. 1, whose complexity is upper bounded by $\mathcal{O}(B(b_1 + 1)N_{\text{train}}2^{b_1+1})$. In fact, Alg. 1 consists of at most $B(b_1 + 1)$ k -means clustering trainings, each with complexity $\mathcal{O}(nkd)$, where n is the number of d -dimensional points and k is the number of clusters [44]. In Alg. 1, we have $n = N_{\text{train}}$, $k \leq 2^{b_1}$ and $d = 2$. Third, the quantization levels are determined through N_P k -means clustering operations on $\mathbf{Z}_{\text{train}}$. The cost of generating $\mathbf{Z}_{\text{train}}$ is $\mathcal{O}(N_A N_C N_P N_{\text{train}})$ while the complexity of the final k -means clustering is $\mathcal{O}(N_P N_{\text{train}} 2^{b_1+1})$. These operations are all performed offline at the BS. During the online deployment, the complexity is simply given by $\mathcal{O}(N_A N_C N_P)$ both at the encoder and at the decoder side.

IV. OFFLOADING OVERHEAD-AWARE CSI FEEDBACK DESIGN

When using a DL-based or PCA-based CSI feedback strategy, the relevant model parameters need to be offloaded from the BS to the UE after the training phase. In the case of DL-based CSI feedback, these parameters are the weights of the neurons composing the deep architecture involved. In the case of PCA-based CSI feedback, these parameters are the element of the complex matrix \mathbf{V}_{N_P} and the complex vector $\boldsymbol{\mu}_{\text{train}}$. Additionally, in both cases, the actual feedback is a quantized version of the compressed channel. When k -means clustering is used to minimize the MSE, also the optimal quantization levels need to be offloaded from the BS to the UE. This necessary offloading process causes an additional overhead in the transmission. Thus, it is crucial to design a CSI feedback strategy being aware that this overhead should be minimum. In this section, we propose two modifications to our PCA-based CSI feedback strategy to reduce the number of offloaded variables. The first modification reduces the number of offloaded PCA parameters, while the second reduces the number of offloaded k -means clustering levels.

A. Reduction of the Number of Offloaded Model Parameters

In our PCA-based CSI feedback as proposed in Section III, the UE needs \mathbf{V}_{N_P} in order to compress the channel along the first N_P principal components. Thus, the number of real model parameters which are offloaded is

$$N_O^{\text{model}} = 2N_A N_C N_P + 2N_A N_C, \quad (13)$$

where the two additive terms are respectively due to the complex matrix \mathbf{V}_{N_P} and the complex vector $\boldsymbol{\mu}_{\text{train}}$. To decrease this number, we observe that the principal components can be sparsified in the angular-delay domain. Let us now consider the general case in which the BS is a uniform planar array (UPA)

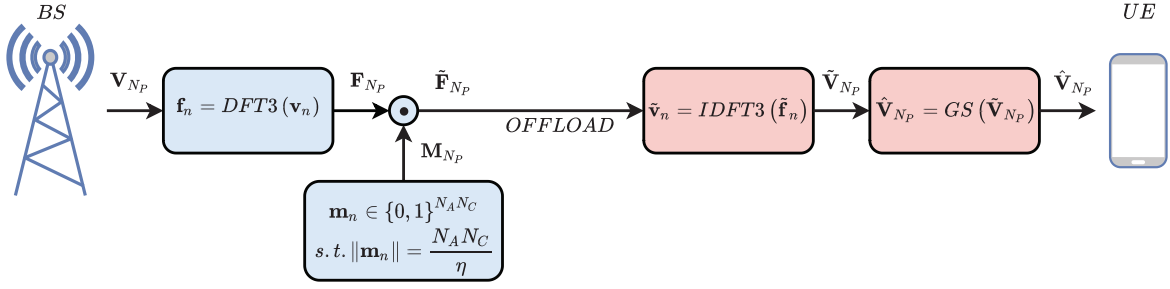


Fig. 2. Model parameters offload from the BS to the UE.

with dimensions $N_X \times N_Y$, where $N_X N_Y = N_A$. Here, we define $\mathbf{v}_n \in \mathbb{C}^{N_A N_C \times 1}$ as the n -th principal component, i.e., the n -th column of \mathbf{V}_{N_P} . This vector \mathbf{v}_n can be reshaped into a tensor of dimensions $N_X \times N_Y \times N_C$ in order to highlight its two spatial and frequency domains. We denote the vectorized 3-dimensional discrete Fourier transform (DFT3) of such a tensor as $\mathbf{f}_n \in \mathbb{C}^{N_A N_C \times 1}$. Thus, \mathbf{f}_n turns out to be sparse since it contains the information of \mathbf{v}_n in the two angular and delay domains. In this way, each principal component \mathbf{v}_n can be approximately reconstructed by considering only the significantly non-zero entries of \mathbf{f}_n .

To decrease the number of offloaded model parameters by exploiting this sparsity property, we introduce a new design parameter η , such that only a fraction $1/\eta$ of all the \mathbf{f}_n entries is offloaded, with $\eta \in [1, N_A N_C]$. In detail, let us define the binary mask vector $\mathbf{m}_n \in \{0, 1\}^{N_A N_C \times 1}$, containing $\frac{N_A N_C}{\eta}$ ones in correspondence of the largest values in \mathbf{f}_n .² To retain only the most significant $\frac{N_A N_C}{\eta}$ values from \mathbf{f}_n , we consider the Hadamard product $\tilde{\mathbf{f}}_n = \mathbf{f}_n \odot \mathbf{m}_n$. Thus, the sparse vector $\tilde{\mathbf{f}}_n$ is offloaded from the BS to the UE instead of \mathbf{v}_n . In matrix form, we have that $\tilde{\mathbf{F}}_{N_P} = \mathbf{F}_{N_P} \odot \mathbf{M}_{N_P}$ is offloaded instead of \mathbf{V}_{N_P} , where $\tilde{\mathbf{F}}_{N_P} = [\tilde{\mathbf{f}}_1, \dots, \tilde{\mathbf{f}}_{N_P}]$, $\mathbf{F}_{N_P} = [\mathbf{f}_1, \dots, \mathbf{f}_{N_P}]$, and $\mathbf{M}_{N_P} = [\mathbf{m}_1, \dots, \mathbf{m}_{N_P}]$.

At the UE side, each vector $\tilde{\mathbf{f}}_n$ is firstly reshaped into a tensor of dimensions $N_X \times N_Y \times N_C$. Then, each principal component $\tilde{\mathbf{v}}_n$ is obtained by vectorizing the 3-dimensional inverse discrete Fourier transform (IDFT3) of such a tensor. Note that the resulting matrix $\tilde{\mathbf{V}}_{N_P} = [\tilde{\mathbf{v}}_1, \dots, \tilde{\mathbf{v}}_{N_P}]$ is nearly semi-unitary, i.e., $\tilde{\mathbf{V}}_{N_P}^H \tilde{\mathbf{V}}_{N_P} \approx \mathbf{I}$, but not semi-unitary since the least significant entries in \mathbf{F}_{N_P} have been pruned to reduce the offloading overhead. For this reason, a last step is needed to ensure that the reconstructed principal component matrix $\hat{\mathbf{V}}_{N_P} = [\hat{\mathbf{v}}_1, \dots, \hat{\mathbf{v}}_{N_P}]$ is semi-unitary, i.e., $\hat{\mathbf{v}}_n \perp \hat{\mathbf{v}}_m \forall n \neq m$ and $\|\hat{\mathbf{v}}_n\| = 1 \forall n$. This is achieved by applying the Gram-Schmidt process to the columns of

$\tilde{\mathbf{V}}_{N_P}$ yielding $\hat{\mathbf{V}}_{N_P} = GS(\tilde{\mathbf{V}}_{N_P})$.³ To summarize, the proposed modification to reduce the number of offloaded model parameters is graphically represented in Fig. 2.

The channel embedding \mathbf{z}_{DL} is now computed at the UE using $\hat{\mathbf{V}}_{N_P}$ instead of the exact matrix \mathbf{V}_{N_P} . Thus, the optimal bit allocation and the quantization levels should also be computed at the BS using the training set projection onto $\hat{\mathbf{V}} = [\hat{\mathbf{v}}_1, \dots, \hat{\mathbf{v}}_{N_A N_C}]$. To this end, all the aforementioned operations are applied at the BS as part of the offline training process. More precisely, after the matrix \mathbf{V} is computed with PCA, it is directly transformed into $\hat{\mathbf{V}}$ by applying the aforementioned operations. The only difference with the process depicted in Fig. 2 is that in this case the operations are not limited to the first N_P principal components. Subsequently, $\hat{\mathbf{G}}_{\text{train}} = \mathbf{H}_{\text{train}} \hat{\mathbf{V}}$ is used in Alg. 1 instead of $\mathbf{G}_{\text{train}}$ to compute the optimal bit allocation and N_P . In addition, $\hat{\mathbf{Z}}_{\text{train}} = \mathbf{H}_{\text{train}} \hat{\mathbf{V}}_{N_P}$ is used to find the optimal quantization levels with k -means clustering instead of $\mathbf{Z}_{\text{train}}$.

With this modification, the number of offloaded real model parameters is reduced to

$$N_O^{\text{model}} = 2 \frac{N_A N_C}{\eta} N_P + \frac{N_A N_C}{\eta} N_P + 2 N_A N_C, \quad (14)$$

where the three additive terms are respectively due to the non-zero complex elements of $\tilde{\mathbf{F}}_{N_P}$, the positions of these elements within $\tilde{\mathbf{F}}_{N_P}$, and the complex vector $\boldsymbol{\mu}_{\text{train}}$. Finally, we remark that this modification allows to introduce an adaptive offloading overhead, as a function of η . Thus, η could be designed by the network operator as an adaptive parameter to trade offloading overhead impact with channel reconstruction quality. This degree of freedom is not present in the existing literature where DL architectures are used for CSI feedback.

B. Reduction of the Number of Offloaded k -means Clustering Parameters

Let us now assume that the bit allocation $\mathbf{b} = [b_1, \dots, b_{N_A N_C}]$ and N_P have been designed through Alg. 1

³This Gram-Schmidt process has complexity $\mathcal{O}(N_A N_C N_P^2)$. Since it is needed only during the offline training stage, we assume that it can be performed at the UE with a negligible impact on the energy consumption. Alternatively, this operation can be replaced by computing the orthogonal factor of the polar decomposition of $\tilde{\mathbf{V}}_{N_P}$ as $\hat{\mathbf{V}}_{N_P} = \tilde{\mathbf{V}}_{N_P} (\tilde{\mathbf{V}}_{N_P}^H \tilde{\mathbf{V}}_{N_P})^{-1/2}$, or its first order Taylor approximation as $\hat{\mathbf{V}}_{N_P} = \tilde{\mathbf{V}}_{N_P} - \frac{1}{2} \tilde{\mathbf{V}}_{N_P} (\tilde{\mathbf{V}}_{N_P}^H \tilde{\mathbf{V}}_{N_P} - \mathbf{I})$. Gram-Schmidt has been selected since it has the lowest complexity and the best reconstruction accuracy among the three.

²The wording ‘‘largest’’ is intended in terms of absolute value, since the \mathbf{f}_n elements are complex.

considering B as the maximum feedback length allowed. In our PCA-based CSI feedback as proposed in Section III, the quantization levels are obtained for each principal component, generating N_P codebooks which all need to be offloaded from the BS to the UE. Thus, to allow the UE to generate a feedback of any length less or equal than B , we need to offload a codebook including $\sum_{r=1}^{b_n} 2^r$ complex quantization levels for the n -th principal component. In addition, for any feedback length less or equal than B , the UE needs to know the bit allocation, i.e., how the bits are allocated to the principal components. To provide the UE with all the possible bit allocations, the BS offloads the vector $\mathbf{m} = [m_1, \dots, m_B]$, where m_i is the index of the principal component receiving the i -th bit in Alg. 1. The vector \mathbf{m} is sufficient to describe all the bit allocations with length from 1 to B because of Proposition 1. Eventually, the number of real k -means clustering parameters which are offloaded is

$$N_O^{k\text{-means}} = \left(2 \sum_{n=1}^{N_P} \sum_{r=1}^{b_n} 2^r \right) + B, \quad (15)$$

where the two additive terms are respectively due to the complex k -means clustering levels and the vector \mathbf{m} .

Now, our goal is to decrease the number of offloaded k -means clustering levels by considering a unique codebook that can be automatically adapted at the UE to fit all the N_P principal components. To this end, we exploit the fact that when a dataset is scaled, also its optimal k -means clustering quantization levels experience the same scaling, as formalized in the following proposition.

Proposition 3. *Let us consider a generic dataset $\mathbf{X} \in \mathbb{R}^{N \times D}$ containing N D -dimensional points, and a real scalar $c > 0$. If the optimal k -means clustering quantization levels of \mathbf{X} are $\{\mathbf{q}_i\}^*$, the optimal k -means clustering quantization levels of the dataset $\mathbf{Y} = c\mathbf{X}$ are $\{\mathbf{q}'_i\}^* = c\{\mathbf{q}_i\}^*$.*

Proof. Please refer to Appendix C. \square

Such a unique codebook is constructed by introducing the matrix $\hat{\mathbf{Z}}_{\text{train}}$, obtained by column-wise dividing $\hat{\mathbf{Z}}_{\text{train}}$ by the vector $\boldsymbol{\sigma} = [\sigma_1, \dots, \sigma_{N_P}]$. In other words, all the columns in $\hat{\mathbf{Z}}_{\text{train}}$ have been normalized in $\hat{\mathbf{Z}}_{\text{train}}$ such that they have unitary variance. Thus, we can now design a codebook which is optimal for all the columns in $\hat{\mathbf{Z}}_{\text{train}}$, assuming that their elements are identically distributed. To do so, we vectorize the matrix $\hat{\mathbf{Z}}_{\text{train}}$ into the vector $\hat{\mathbf{z}}_{\text{train}}$, and we apply k -means clustering to $\hat{\mathbf{z}}_{\text{train}}$ considering $k = 2^r$ with $r \in [1, b_1]$, where b_1 is the first element of \mathbf{b} . We denote the quantization levels of the resulting codebook as $\{\mathbf{q}_i\}^*$. Finally, according to Proposition 3, we obtain the quantization levels for the n -th column of $\hat{\mathbf{Z}}_{\text{train}}$ (i.e., for the n -th principal component) by simply computing $\sigma_n \{\mathbf{q}_i\}^*$.

With this modification, the number of real k -means clustering parameters which are offloaded is given by

$$N_O^{k\text{-means}} = \left(2 \sum_{r=1}^{b_1} 2^r \right) + N_P + B, \quad (16)$$

where the three additive terms are respectively due to the code-

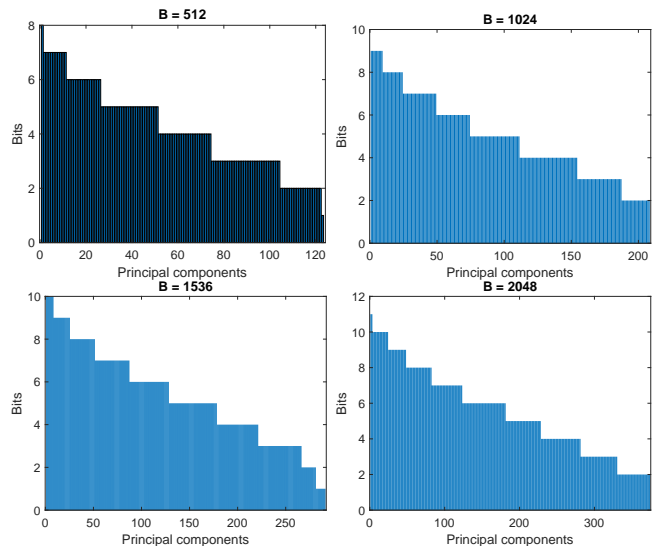


Fig. 3. Bit allocation to the principal components for four different values of B .

book containing the complex quantization levels, the vector $\boldsymbol{\sigma}$ used to adapt the codebook to each principal component, and the vector \mathbf{m} used to obtain the bit allocation.

We finally remark that the number of offloaded parameters considered in this section is to be intended per user. Nevertheless, in multi-user scenarios, this information is common to all the users connected to the BS. Thus, the model parameters and the k -means clustering levels can be broadcasted to all the intended users in these scenarios, without further increasing the offloading overhead.

V. NUMERICAL RESULTS

In this section, we provide numerical results to evaluate our proposed CSI feedback strategy, and compare it with state-of-the-art DL architectures proposed for the same scope. The performance is measured in terms of downlink channel reconstruction quality, assessed by considering four metrics:

- the NMSE between the estimated downlink channel $\hat{\mathbf{H}}_{\text{DL}}$ and the true downlink channel \mathbf{H}_{DL} , defined as

$$NMSE = \frac{\|\hat{\mathbf{H}}_{\text{DL}} - \mathbf{H}_{\text{DL}}\|_F^2}{\|\mathbf{H}_{\text{DL}}\|_F^2}; \quad (17)$$

- the cosine similarity between $\hat{\mathbf{H}}_{\text{DL}}$ and \mathbf{H}_{DL} , defined as

$$\rho = \frac{1}{N_C} \sum_{n_C=1}^{N_C} \frac{|\hat{\mathbf{h}}_{n_C}^H \mathbf{h}_{n_C}|}{\|\hat{\mathbf{h}}_{n_C}\| \|\mathbf{h}_{n_C}\|}, \quad (18)$$

where $\hat{\mathbf{h}}_{n_C}$ and \mathbf{h}_{n_C} are the n_C -th columns of $\hat{\mathbf{H}}_{\text{DL}}$ and \mathbf{H}_{DL} , respectively;

- the bit error rate (BER) obtained by precoding binary phase shift keying (BPSK) symbols at the BS based on the reconstructed CSI;
- the average sum rate obtained with zero-forcing beamforming and water-filling power allocation.

In addition, we assess the considered CSI feedback strategies in terms of offloading overhead (i.e., the number of offloaded

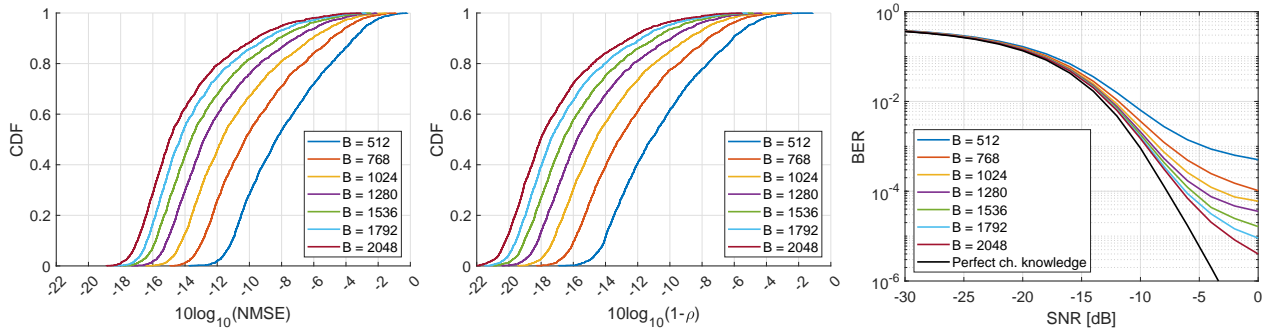


Fig. 4. NMSE CDF (left), cosine similarity CDF (center), and BER (right) for different values of B .

model parameters) and in terms of number of training samples required.

A. Dataset Description

The channels for both training and test sets were generated with QuaDRiGa version 2.4, a MATLAB based statistical ray-tracing channel simulator [45]. To this end, we consider an urban microcell in which single-antenna UEs are uniformly distributed at a distance included in the interval $[20, 100]$ m from the BS, and at a height of 1.5 m over the ground. The links between the BS and the UEs are non-line-of-sight (NLoS), and $L = 58$ paths are considered to simulate a rich multipath environment. The channel model utilized to generate the channel samples is “3GPP_38.901_UMi_NLoS” in QuaDRiGa. The BS, 20 m high, is a UPA composed of $N_A = 64$ antennas. These array elements are arranged on an $N_X \times N_Y$ shape with an antenna spacing of half wavelength, where $N_X = 8$ and $N_Y = 8$. The uplink and downlink center frequencies are $f_{UL} = 2.5$ GHz and $f_{DL} = 2.62$ GHz. In each frequency band, the channel bandwidth is $W = 8$ MHz, divided into $N_C = 160$ OFDM subcarriers. The large-scale fading parameters and the path directions are kept constant over the uplink-downlink frequency gap. On the other hand, the small-scale fading effects depend on the path phase-shifts, in turn dependent on the frequency. Thus, they are in practice uncorrelated over the frequency gap in rich multipath environments.

The channels resulting from the simulations contain the path loss, the large-scale fading, and small-scale fading effects. Thus, in order to work with scaled channels, we normalize the dataset according to

$$\mathbf{H}_{UL} \leftarrow L_{UL}^{-1} \mathbf{H}_{UL}, \mathbf{H}_{DL} \leftarrow L_{DL}^{-1} \mathbf{H}_{DL}, \quad (19)$$

where the scalars L_{UL}^{-1} and L_{DL}^{-1} contain the path loss and the large-scale fading effects. In total, $N = N_{\text{train}} + N_{\text{test}}$ users are randomly dropped in the cell and, for each user, the pair of channels \mathbf{H}_{UL} , \mathbf{H}_{DL} is generated. Firstly, the *offline learning* stage is carried out considering N_{train} noisy uplink channel matrices. Secondly, the performance is tested on N_{test} downlink channel matrices, corresponding to the users not considered during the training phase. We assume that only noisy versions of the channel matrices are available both in the *offline learning* and *online development* stages, with $SNR_{UL} = 10$ dB and $SNR_{DL} = 10$ dB. The ground truth

channels \mathbf{H}_{DL} are only used to evaluate the reconstruction performance. Furthermore, we set $N_{\text{train}} = 5000$ and $N_{\text{test}} = 2000$.

B. Performance Evaluation

We now assess the performance of our PCA-based CSI feedback strategy. Experimentally, we noticed that the two modifications proposed in Section IV do not impact visibly the performance if $\eta \approx 16$ or less. Thus, the performance reported here refers to our proposed CSI feedback strategy including the two modifications with $\eta = 16$, unless otherwise specified. First of all, we inspect how the feedback bits are allocated to the principal components. In Fig. 3, we report a graphical representation of the vector \mathbf{b} resulting from Alg. 1 applied to four different values of B . As expected, we observe that the number of considered principal components N_P and the number of bits assigned to the first principal component b_1 increase as B increases.

Fig. 4 reports the cumulative distribution functions (CDFs) of the NMSE and the cosine similarity ρ between the reconstructed and the true downlink channel matrices. Besides, we plot the BER obtained in downlink by precoding uncoded BPSK symbols according to the reconstructed CSI. The CDFs, calculated over the whole test set, and the obtained BER show that the reconstruction quality increases with B , and that, more importantly, no performance upper bound is present. When the BER metric is considered, the only performance upper bound present is given by the BER obtained with perfect CSI. In fact, B could be potentially increased until all the principal components are considered to embed the CSI. In this extreme case, approximately perfect channel reconstruction could be achieved. This property cannot be found in DL strategies recently proposed for CSI feedback. In these strategies, the reconstruction quality is always bounded by the latent space dimensionality, which is fixed regardless of the value of B .

Now, we investigate how the channel reconstruction quality varies according to the antenna number N_A and subcarrier number N_C . To this end, we consider four different CSI dimensions $N_A \times N_C$, namely 32×80 , 32×160 , 64×80 , and 64×160 . We show the reconstruction quality in terms of cosine similarity obtained for these channels when $B = 512$ and $B = 1024$ feedback bits are used in Fig. 5 (left). As expected, the reconstruction quality is higher for CSI matrices with lower dimensionalities. We also observe that the channels

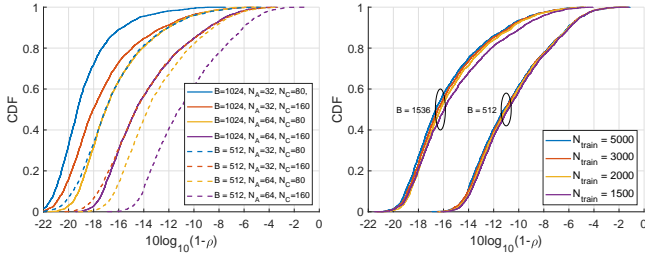


Fig. 5. Cosine similarity CDFs for different CSI dimensions (left) and for different number of training samples (right).

with dimensions 32×160 are better reconstructed than the channels with dimensions 64×80 , despite these two types of channel matrices have the same number of entries. The reason is that frequency correlation is higher than spatial correlation in an OFDM channel matrix, as also noticed in [19]. Thus, the information along the frequency dimension can be compressed more efficiently.

A problem concerning ML approaches is the need of training samples. Experimentally, we observe that $N_{\text{train}} = 5000$ training samples are necessary to well-train both PCA and k -means clustering. For this reason, this is the number of training samples used to present the obtained results in the manuscript. However, we explore now the performance degradation experienced when this number is lowered. In Fig. 5 (right), the CDF of the cosine similarity obtained with different values of N_{train} is reported. We observe that the reconstruction quality only slightly degrades when $B = 1536$, while it remains approximately stable when the number of bits employed is low, i.e., $B = 512$. This means that the principal components are well reconstructed even with less training samples. However, k -means clustering is the bottleneck that precludes the use of a lower N_{train} , especially when the number of quantization levels is high.

Finally, we report the performance of multi-user precoding carried out with the reconstructed downlink channel matrices. More precisely, we use the reconstructed downlink channels to serve $K = 8$ UEs through zero-forcing beamforming with water-filling power allocation. Zero-forcing beamforming is applied independently to each subcarrier and the resulting sum rate is averaged over the N_C subcarriers. The water-filling power allocation is designed assuming that the reconstructed downlink channel is the perfect channel. Thus, the multi-user interference is not captured in the water-filling solution. In order to obtain reliable results, Monte Carlo simulations are run by randomly selecting, in each simulation, $K = 8$ downlink channels among the N_{test} available in the test set. Fig. 6 reports the average sum rate obtained by compressing the CSI with four different feedback lengths B . Here, our CSI feedback strategy, namely “PCA”, is compared with two baseline strategies based on DL architectures. “AE” is the convolutional autoencoder proposed in [18], while “CsiNet-Pro” is the architecture proposed in [28]. In addition, the learning-based results are compared with the classical theory-based approach “IDFT”, also used for comparison in [18]. According to the “IDFT” approach, the noisy CSI $\tilde{\mathbf{H}}_{\text{DL}}$ is

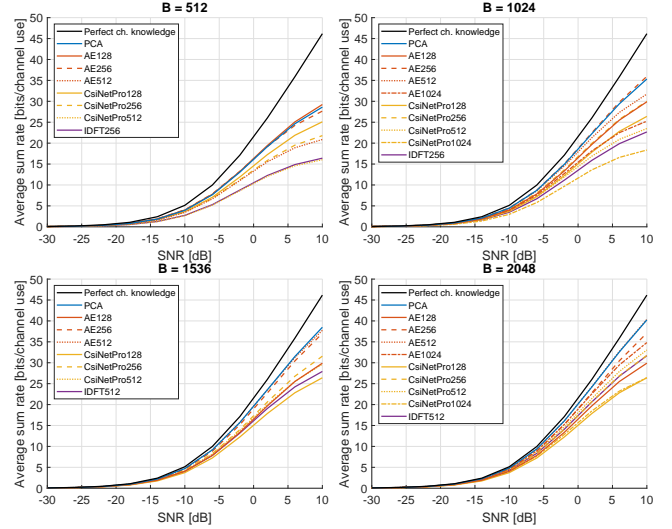


Fig. 6. Average sum rate with zero-forcing beamforming for four different values of B . “PCA” has been trained with 2000 samples, “AE” and “CsiNet-Pro” have been trained with 40000 samples.

firstly transformed into the space-delay domain through a 2-dimensional inverse discrete Fourier transform (IDFT2). Then, only the elements of the first columns of the resulting matrix are considered for the feedback. At the BS, the CSI is reconstructed through a zero-padding operation followed by a 2-dimensional discrete Fourier transform (DFT2). Note that depending on how many columns are retained, the CSI can be compressed into latent spaces with different dimensionalities. For these three baselines, the number in the legend name denotes the latent space dimensionality. For conciseness, in Fig. 6 we report the performance of “IDFT” applied with the best latent space dimensionality for each B .

For the baseline strategies, the feedback bits are allocated uniformly to all the latent space dimensions, and the quantization levels are determined with k -means clustering⁴. Preliminary experiments confirmed that $N_{\text{train}} = 5000$ training samples are not enough to well-train the “AE” and “CsiNet-Pro” architectures. With this amount of training data, these DL architectures are not able to learn an expressive representation of the channels in the latent space. For this reason, in Fig. 6, we report the performance of well-trained “AE” and “CsiNet-Pro” architectures, i.e., trained with 40000 training samples.

From Fig. 6, we notice that the learning-based solutions always outperform “IDFT”. Among the two considered DL architectures, “AE” outperforms “CsiNetPro” for every considered B , as already highlighted in [18]. Furthermore, for the DL architectures, we notice that there is not a unique latent space dimensionality N_L that is optimal for every feedback length B . This result supports our intuition that N_L should be designed according to the number of bits B . Since we consider such an adaptive design, our strategy “PCA” performs approximately as the best autoencoder “AE” in every B considered. Thus,

⁴The proposed bit allocation strategy could be applied also to DL architectures. However, in these architectures, the compressed CSI entries are approximately identically distributed for all latent space dimensions. For this reason, the proposed bit allocation applied to autoencoders boils down to uniform bit allocation, with no visible improvement with respect to the latter.

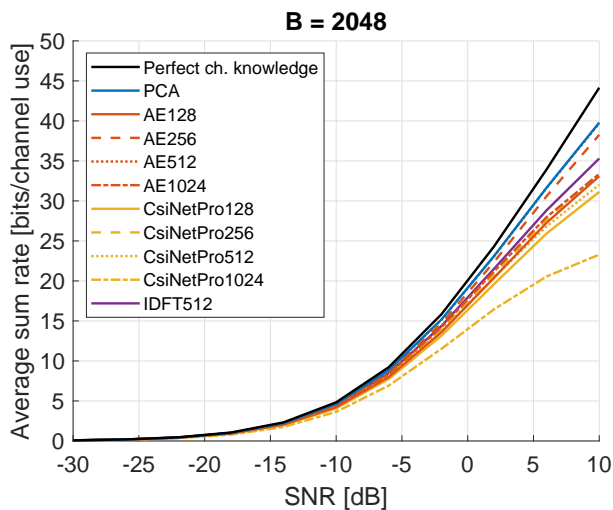


Fig. 7. Average sum rate with zero-forcing beamforming for $B = 2048$. The ML models have been trained on urban microcell channel samples and tested on rural macrocell channels.

PCA can be successfully applied to compress the channel matrix with a significantly reduced training set.

In this study and in the related literature, it is assumed that the trained ML algorithm is used to compress channel matrices with the same fading distribution as seen during the training session. However, when the channel statistics vary, the CSI feedback strategy should be able to compress differently distributed channels before an updated trained model becomes available. To explore the performance under different channel models, we train our PCA-based approach and the baseline DL architectures on uplink channel samples drawn from the urban microcell scenario “3GPP_38.901_UMi_NLOS”. After this training session, we test the CSI feedback methods on downlink channel samples drawn from the rural macrocell scenario “3GPP_38.901_RMa_NLOS”. Note that the multipath in the latter environment is less severe than in the former, since only $L = 11$ paths are considered by the QuaDRiGa simulator. The only elements in common between the training and testing scenarios are the number of antennas and subcarriers, the bandwidth and the center frequencies of uplink and downlink bands. The obtained sum rate is reported in Fig. 7, for $B = 2048$. Fig. 7 shows that the knowledge obtained in a rich multipath environment can be successfully reused to compress sparser CSI matrices. Our PCA-based strategy performs as the best “AE” architecture, i.e., “AE512”, and largely outperforms “CsiNetPro” and “IDFT512” baselines.

To analyze the effect of the parameter η on the performance, we plot the average sum rate versus the feedback length B , by fixing the signal-to-noise ratio (SNR) experienced by each of the K user to 10 dB. In Fig. 8, the performance of our strategy is compared with the two considered baseline DL architectures, each with four different N_L . We notice that the performance of each DL architecture saturates as B increases due to the fixed latent space dimensionality. Thus, each N_L turns out to be optimal only for some specific values of B . More precisely, “AE128” is the best autoencoder when $B = 512$, “AE256” is preferred when $B \in \{768, 1024, 1280\}$, while

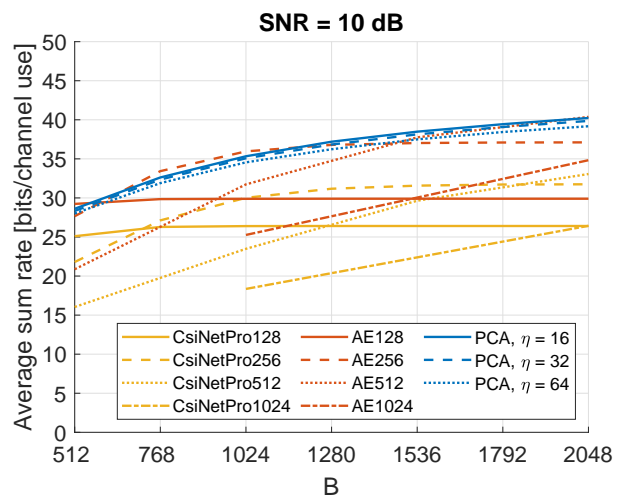


Fig. 8. Average sum rate with zero-forcing beamforming vs feedback length B , with SNR = 10 dB at each UE. “PCA” has been trained with 2000 samples, “AE” and “CsiNetPro” have been trained with 40000 samples.

“AE512” is the autoencoder achieving the highest average sum rate when $B \in \{1536, 1792, 2048\}$. The four “CsiNetPro” achieve a lower average sum rate than their respective “AE” architectures. Conversely, the performance of our PCA-based strategy with $\eta = 16$ is comparable with the one of the best autoencoder “AE” for each value of B . We notice that the performance deterioration caused by increasing η is minimal.

C. Offloading Impact

We now analyze the impact of the two modifications proposed in Section IV on the overhead caused by parameter offloading. The effect of the first modification can be analyzed by comparing (13) with (14). When computing N_O^{model} , the number of offloaded parameters due to μ_{train} can be neglected, since in practice $N_P \gg 1$. Thus, we have that the first modification decreases the number of offloaded model parameters of approximately $\frac{2}{3}\eta$ times. In our numerical scenario, $B = 2048$ yields $N_P = 374$. Hence, without the first modification, we have $N_O^{\text{model}} = 7.68 \times 10^6$ according to (13). Conversely, when the first modification is applied with $\eta = 16$, N_O^{model} is reduced to 0.739×10^6 according to (14).

Considering the offloaded k -means clustering parameters, the effect of the second modification is given by comparing (15) with (16). Also to quantify the effect of the second modification, we refer to the case in which the maximum feedback length allowed is $B = 2048$, yielding $N_P = 374$ and $b_1 = 11$ in our numerical scenario. Without the second modification, we have $N_O^{k\text{-means}} = 243 \times 10^3$ according to (15). Conversely, when the second modification is applied, $N_O^{k\text{-means}}$ is reduced to 10.6×10^3 according to (16).

When both modifications are applied, we notice that $N_O^{\text{model}} \gg N_O^{k\text{-means}}$. Thus, now we compare our PCA-based CSI feedback strategy with the two baseline DL-based strategies in terms of offloaded model parameters, neglecting the offloaded k -means clustering parameters. This comparison is carried out in Fig. 9, where N_O^{model} is reported for our strategy when both modifications are considered, with

TABLE I
PERFORMANCE COMPARISON WITH FEEDBACK LENGTH $B = 2048$.

	Average sum rate [bits/channel use]	Number of offloaded model parameters	Number of training samples
PCA, $\eta = 16$	40.2	0.739×10^6	5×10^3
PCA, $\eta = 32$	39.9	0.387×10^6	5×10^3
PCA, $\eta = 64$	39.2	0.211×10^6	5×10^3
AE	40.4	1.45×10^6	40×10^3
CsiNetPro	33.1	7.37×10^6	40×10^3

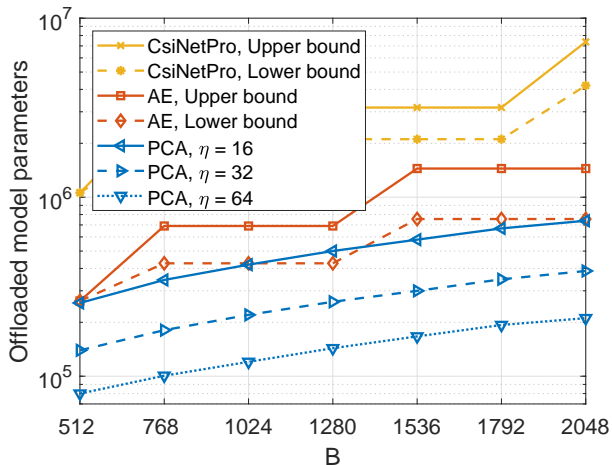


Fig. 9. Number of offloaded model parameters vs feedback length B . “PCA” has been trained with 2000 samples, “AE” and “CsiNetPro” have been trained with 40000 samples.

$\eta \in \{16, 32, 64\}$. For the two considered DL architectures, an upper bound and a lower bound on the number of offloaded model parameters are reported. The upper bound represents the case in which we offload all the necessary encoders to generate a feedback of length less or equal than B . These encoders can be retrieved from Fig. 8, considering only the most performing ones for feedback lengths less or equal than B . The lower bound represents the case in which we apply the parallel multiple-rate framework proposed in [27]. In this framework, among the necessary encoders, only the encoder with the largest latent space dimensionality is offloaded. The other encoders are obtained at the UE by just considering a reduced number of latent space dimensions from this encoder. Note that this framework inevitably causes a slight degradation in the channel reconstruction performance, as stated in [27], that is not assessed in this study. We remark that the parameter number of DL models can be reduced at the cost of a performance degradation with techniques such as pruning and knowledge distillation. However, to offer a clear comparison in terms of both reconstruction performance and offloading overhead, we do not alter the architectures proposed in [18], [28].

Fig. 9 shows that our strategy is convenient also in terms of offloading overhead compared with the two DL-based strategies, not only in terms of training samples required. When $\eta = 16$, our strategy and the “AE” strategy used with the

framework proposed in [27] cause similar offloading overhead. However, it is possible to significantly reduce this overhead of our strategy by only slightly affecting the reconstruction performance thanks to the adaptive parameter η .

Finally, in Tab I we summarize the comparison between our PCA-based strategy and the two considered DL-based strategies, for a feedback length $B = 2048$. Here, the offloaded parameter number for the deep architectures are computed without considering the framework in [27], since it would cause a non-negligible performance degradation. Compared to “AE”, our strategy using $\eta = 16$ halves the offloading overhead and reduces the number of training samples by eight times. If $\eta = 64$ is considered, the offloading overhead is reduced by 6.87 times, at the cost of a 2.97% average sum rate loss. Compared to “CsiNetPro”, our strategy improves the average sum rate by 21.7% (resp. 18.5%), and reduces the offloading overhead by 10.0 (resp. 34.9) times, when $\eta = 16$ (resp. $\eta = 64$). Considering maximum feedback lengths ranging from $B = 521$ to $B = 2048$, our strategy used with $\eta = 64$ improves the sum rate by 17% on average, and reduces the offloading overhead by 23.4 times compared to “CsiNetPro”.

VI. CONCLUSION

In this study, we propose a novel strategy to design the CSI feedback in FDD massive MIMO systems. This strategy allows to design the feedback with variable length, while reducing the number of parameter offloaded from the BS to the UE. Firstly, the channel is compressed using PCA, with a latent space dimensionality adapted to the number of available feedback bits. Then, the feedback bits are allocated to the principal components by minimizing a properly defined NMSE distortion. Finally, the quantization levels are determined with k -means clustering. In addition, we allow an adaptive number of offloaded model parameters, which can be adjusted to trade offloading overhead and CSI reconstruction quality. Such an adaptive offloading overhead has been never considered in previous literature employing DL approaches.

Through simulations, we compare our strategy with state-of-the-art DL architectures proposed for the same scope. Numerical results show that our strategy performs better or approximately equal, to DL architectures well-trained on larger datasets, in terms of sum rate obtained with multi-user precoding. The offloading overhead can be significantly reduced in our strategy, with approximately no impact on the

CSI reconstruction. At the same time, PCA is characterized by a lightweight training phase, requiring a reduced number of training samples. This lightweight training phase enables, in practical developments, more frequent trainings. In this way, the compression strategy could be better maintained updated, as the environment evolves in time. Compared to “CsiNetPro”, our strategy using $\eta = 64$ improves the sum rate by 17% on average, reduces the offloading overhead by 23.4 times, and requires eight times fewer training parameters.

APPENDIX

A. Proof of Proposition 1

Since the bit allocation $\mathbf{b}' = [b'_1, \dots, b'_{N_{A}N_C}]$ contains one more bit than $\mathbf{b} = [b_1, \dots, b_{N_{A}N_C}]$, there is always a principal component m such that $b'_m = b_m + C$, with $C \geq 1$. Thus, to prove Proposition 1, we need to prove that the bit allocation $[b_1, \dots, b_m + 1, \dots, b_{N_{A}N_C}]$ is better than any other allocation of $B + 1$ bits $[b'_1, \dots, b_m + C, \dots, b'_{N_{A}N_C}]$. This is equivalent to saying that the distortion caused by $[b_1, \dots, b_m + 1, \dots, b_{N_{A}N_C}]$ is less than the distortion caused by $[b'_1, \dots, b_m + C, \dots, b'_{N_{A}N_C}]$, that is

$$\begin{aligned} & d_1(b_1) + \dots + d_m(b_m + 1) + \dots + d_{N_{A}N_C}(b_{N_{A}N_C}) \\ & < d_1(b'_1) + \dots + d_m(b_m + C) + \dots + d_{N_{A}N_C}(b'_{N_{A}N_C}) \end{aligned} \quad (20)$$

For convenience, we rewrite (20) as

$$\begin{aligned} & [d_1(b_1) + \dots + d_m(b_m) + \dots + d_{N_{A}N_C}(b_{N_{A}N_C})] \\ & \quad + [d_m(b_m + 1) - d_m(b_m)] \\ & < [d_1(b'_1) + \dots + d_m(b_m + C - 1) + \dots + d_{N_{A}N_C}(b'_{N_{A}N_C})] \\ & \quad + [d_m(b_m + C) - d_m(b_m + C - 1)], \end{aligned} \quad (21)$$

where two additive terms are highlighted in both sides of the inequality. Thus, (21) can be proved by independently verifying the following two inequalities

$$\begin{aligned} & d_1(b_1) + \dots + d_m(b_m) + \dots + d_{N_{A}N_C}(b_{N_{A}N_C}) \\ & < d_1(b'_1) + \dots + d_m(b_m + C - 1) + \dots + d_{N_{A}N_C}(b'_{N_{A}N_C}) \end{aligned} \quad (22)$$

$$d_m(b_m + 1) - d_m(b_m) \leq d_m(b_m + C) - d_m(b_m + C - 1). \quad (23)$$

Firstly, (22) holds since $\mathbf{b} = [b_1, \dots, b_{N_{A}N_C}]$ is the optimal bit allocation of B bits. Thus, any other allocation of B bits $[b'_1, \dots, b_m + C - 1, \dots, b'_{N_{A}N_C}]$ causes an higher distortion. Secondly, to prove (23), we resort to an explicit expression of the MSE distortion as a function of the bit number. Since such a distortion in the case of k -means clustering is not available in close form, we consider the distortion-rate function, which provides a lower bound on the MSE distortion [46]. According to information theory, the distortion-rate function of a CSCG random variable $X_n \sim \mathcal{CN}(0, \sigma_n^2)$ quantized with b_n bits is given by $d_n(b_n) = \sigma_n^2 2^{-b_n}$ [46]. Thus, assuming that on the n -th principal component the training set is distributed as

$\mathcal{CN}(0, \sigma_n^2)$, (23) becomes

$$\sigma_m^2 2^{-(b_m+1)} - \sigma_m^2 2^{-b_m} \leq \sigma_m^2 2^{-(b_m+C)} - \sigma_m^2 2^{-(b_m+C-1)} \quad (24)$$

$$\sigma_m^2 2^{-b_m} (2^{-1} - 1) \leq \sigma_m^2 2^{-(b_m+C-1)} (2^{-1} - 1), \quad (25)$$

which is verified since $C \geq 1$ implies $2^{-b_m} \geq 2^{-(b_m+C-1)}$.

B. Proof of Proposition 2

To prove Proposition 2, we prove that the optimal b_n cannot be greater than b_{n-1} since the bit allocation $b_{n-1} = C + \Delta C$, $b_n = C$ is always better than $b_{n-1} = C$, $b_n = C + \Delta C$, where $C \in \mathbb{N}$, $\Delta C \in \mathbb{N}^*$. This means that

$$d_{n-1}(C + \Delta C) + d_n(C) < d_{n-1}(C) + d_n(C + \Delta C), \quad (26)$$

since the best bit allocation to the two principal components $n - 1$ and n is the one that minimizes the distortion $d_{n-1} + d_n$. As in Appendix A, we write the distortion caused by quantizing the n -th principal component with b_n bits as $d_n(b_n) = \sigma_n^2 2^{-b_n}$. Thus, (26) can be rewritten as

$$\sigma_{n-1}^2 2^{-(C+\Delta C)} + \sigma_n^2 2^{-C} < \sigma_{n-1}^2 2^{-C} + \sigma_n^2 2^{-(C+\Delta C)} \quad (27)$$

$$\sigma_n^2 2^{-C} - \sigma_n^2 2^{-(C+\Delta C)} < \sigma_{n-1}^2 2^{-C} - \sigma_{n-1}^2 2^{-(C+\Delta C)} \quad (28)$$

$$\sigma_n^2 2^{-C} (1 - 2^{-\Delta C}) < \sigma_{n-1}^2 2^{-C} (1 - 2^{-\Delta C}), \quad (29)$$

which is verified since the principal components are ordered, i.e., $\sigma_n^2 < \sigma_{n-1}^2$.

C. Proof of Proposition 3

k -means clustering groups the N dataset points into k clusters, each assigned to a unique quantization level. This is done by minimizing the sum of the square distances between each data point and the quantization level assigned to its cluster [41]. Let us denote with \mathbf{x}_n the n -th point in the dataset \mathbf{X} . The k -means clustering process can be formalized by introducing the binary indicator $r_{ni} \in \{0, 1\}$ such that $r_{ni} = 1$ if \mathbf{x}_n is assigned to the i -th cluster, and $r_{ni} = 0$ otherwise. The optimal clustering indicators $\{r_{ni}\}^*$ and quantization levels $\{\mathbf{q}_i\}^*$ are given by

$$\{r_{ni}\}^*, \{\mathbf{q}_i\}^* = \min_{\{r_{ni}\}, \{\mathbf{q}_i\}} \sum_{n=1}^N \sum_{i=1}^k r_{ni} \|\mathbf{x}_n - \mathbf{q}_i\|^2. \quad (30)$$

Now, let us consider the scaled dataset $\mathbf{Y} = c\mathbf{X}$, in which \mathbf{y}_n is the n -th point. In this case, the optimal clustering indicators $\{r'_{ni}\}^*$ and quantization levels $\{\mathbf{q}'_i\}^*$ are

$$\{r'_{ni}\}^*, \{\mathbf{q}'_i\}^* = \min_{\{r'_{ni}\}, \{\mathbf{q}'_i\}} \sum_{n=1}^N \sum_{i=1}^k r'_{ni} \|\mathbf{y}_n - \mathbf{q}'_i\|^2 \quad (31)$$

$$= \min_{\{r'_{ni}\}, \{\mathbf{q}'_i\}} \sum_{n=1}^N \sum_{i=1}^k r'_{ni} \|c\mathbf{x}_n - \mathbf{q}'_i\|^2 \quad (32)$$

$$= \min_{\{r'_{ni}\}, \{\mathbf{q}'_i\}} \sum_{n=1}^N \sum_{i=1}^k r'_{ni} \left\| \mathbf{x}_n - \frac{1}{c} \mathbf{q}'_i \right\|^2, \quad (33)$$

where the objective function in (32) has been multiplied by the scalar c^{-2} to obtain (33). Noting that the problem in (33) is

equal to (30), it holds $\{r'_{ni}\}^* = \{r_{ni}\}^*$ and $\frac{1}{c}\{\mathbf{q}'_i\}^* = \{\mathbf{q}_i\}^*$. Thus, we verified that $\{\mathbf{q}'_i\}^* = c\{\mathbf{q}_i\}^*$.

REFERENCES

- [1] B. Clerckx and C. Oestges, *MIMO wireless networks: Channels, techniques and standards for multi-antenna, multi-user and multi-cell systems*. Academic Press, 2013.
- [2] D. J. Love, R. W. Heath, V. K. N. Lau, D. Gesbert, B. D. Rao, and M. Andrews, "An overview of limited feedback in wireless communication systems," *IEEE J. Sel. Areas Commun.*, vol. 26, no. 8, pp. 1341–1365, 2008.
- [3] J. Choi, D. J. Love, and P. Bidigare, "Downlink training techniques for FDD massive MIMO systems: Open-loop and closed-loop training with memory," *IEEE J. Sel. Topics Signal Process.*, vol. 8, no. 5, pp. 802–814, 2014.
- [4] X. Rao and V. K. N. Lau, "Distributed compressive CSIT estimation and feedback for FDD multi-user massive MIMO systems," *IEEE Trans. Signal Process.*, vol. 62, no. 12, pp. 3261–3271, 2014.
- [5] Z. Gao, L. Dai, Z. Wang, and S. Chen, "Spatially common sparsity based adaptive channel estimation and feedback for FDD massive MIMO," *IEEE Trans. Signal Process.*, vol. 63, no. 23, pp. 6169–6183, 2015.
- [6] A. Adhikary, J. Nam, J.-Y. Ahn, and G. Caire, "Joint spatial division and multiplexing-the large-scale array regime," *IEEE Trans. Inf. Theory*, vol. 59, no. 10, pp. 6441–6463, 2013.
- [7] Y. Xu, G. Yue, and S. Mao, "User grouping for massive MIMO in FDD systems: New design methods and analysis," *IEEE Access*, vol. 2, pp. 947–959, 2014.
- [8] M. Dai, B. Clerckx, D. Gesbert, and G. Caire, "A rate splitting strategy for massive MIMO with imperfect CSIT," *IEEE Trans. Wireless Commun.*, vol. 15, no. 7, pp. 4611–4624, 2016.
- [9] M. Alrabeiah and A. Alkhateeb, "Deep learning for TDD and FDD massive MIMO: Mapping channels in space and frequency," in *2019 53rd Asilomar Conference on Signals, Systems, and Computers*, 2019, pp. 1465–1470.
- [10] M. Arnold, S. Dörner, S. Cammerer, S. Yan, J. Hoydis, and S. t. Brink, "Enabling FDD massive MIMO through deep learning-based channel prediction," *arXiv preprint arXiv:1901.03664*, 2019.
- [11] Y. Yang, F. Gao, G. Y. Li, and M. Jian, "Deep learning-based downlink channel prediction for FDD massive MIMO system," *IEEE Commun. Lett.*, vol. 23, no. 11, pp. 1994–1998, 2019.
- [12] P. Dong, H. Zhang, G. Y. Li, N. NaderiAlizadeh, and I. S. Gaspar, "Deep CNN for wideband mmwave massive MIMO channel estimation using frequency correlation," in *ICASSP 2019 - 2019 IEEE International Conference on Acoustics, Speech and Signal Processing (ICASSP)*, 2019, pp. 4529–4533.
- [13] Y. Han, M. Li, S. Jin, C.-K. Wen, and X. Ma, "Deep learning-based FDD non-stationary massive MIMO downlink channel reconstruction," *IEEE J. Sel. Areas Commun.*, vol. 38, no. 9, pp. 1980–1993, 2020.
- [14] M. S. Safari, V. Pourahmadi, and S. Sodagari, "Deep UL2DL: Data-driven channel knowledge transfer from uplink to downlink," *IEEE Open Journal of Vehicular Technology*, vol. 1, pp. 29–44, 2020.
- [15] J. Wang, Y. Ding, S. Bian, Y. Peng, M. Liu, and G. Gui, "UL-CSI data driven deep learning for predicting DL-CSI in cellular FDD systems," *IEEE Access*, vol. 7, pp. 96 105–96 112, 2019.
- [16] V. Rizzello, I. Brayek, M. Joham, and W. Utschick, "Learning the channel state information across the frequency division gap in wireless communications," in *WSA 2020; 24th International ITG Workshop on Smart Antennas*, 2020, pp. 1–6.
- [17] J. Guo, C.-K. Wen, and S. Jin, "CANet: Uplink-aided downlink channel acquisition in FDD massive MIMO using deep learning," *IEEE Trans. Commun.*, pp. 1–1, 2021.
- [18] V. Rizzello and W. Utschick, "Learning the CSI denoising and feedback without supervision," in *2021 IEEE 22nd International Workshop on Signal Processing Advances in Wireless Communications (SPAWC)*, 2021, pp. 16–20.
- [19] C.-K. Wen, W.-T. Shih, and S. Jin, "Deep learning for massive MIMO CSI feedback," *IEEE Wireless Commun. Lett.*, vol. 7, no. 5, pp. 748–751, 2018.
- [20] Z. Liu, L. Zhang, and Z. Ding, "Exploiting bi-directional channel reciprocity in deep learning for low rate massive MIMO CSI feedback," *IEEE Wireless Commun. Lett.*, vol. 8, no. 3, pp. 889–892, 2019.
- [21] —, "An efficient deep learning framework for low rate massive MIMO CSI reporting," *IEEE Trans. Commun.*, vol. 68, no. 8, pp. 4761–4772, 2020.
- [22] M. B. Mashhadi, Q. Yang, and D. Gündüz, "Distributed deep convolutional compression for massive MIMO CSI feedback," *IEEE Trans. Wireless Commun.*, vol. 20, no. 4, pp. 2621–2633, 2021.
- [23] Z. Cao, W.-T. Shih, J. Guo, C.-K. Wen, and S. Jin, "Lightweight convolutional neural networks for CSI feedback in massive MIMO," *IEEE Commun. Lett.*, vol. 25, no. 8, pp. 2624–2628, 2021.
- [24] Y. Sun, W. Xu, L. Liang, N. Wang, G. Y. Li, and X. You, "A lightweight deep network for efficient CSI feedback in massive MIMO systems," *IEEE Wireless Commun. Lett.*, vol. 10, no. 8, pp. 1840–1844, 2021.
- [25] S. Jo and J. So, "Adaptive lightweight CNN-based CSI feedback for massive MIMO systems," *IEEE Wireless Commun. Lett.*, vol. 10, no. 12, pp. 2776–2780, 2021.
- [26] T. Wang, C.-K. Wen, S. Jin, and G. Y. Li, "Deep learning-based CSI feedback approach for time-varying massive MIMO channels," *IEEE Wireless Commun. Lett.*, vol. 8, no. 2, pp. 416–419, 2019.
- [27] J. Guo, C.-K. Wen, S. Jin, and G. Y. Li, "Convolutional neural network-based multiple-rate compressive sensing for massive MIMO CSI feedback: Design, simulation, and analysis," *IEEE Trans. Wireless Commun.*, vol. 19, no. 4, pp. 2827–2840, 2020.
- [28] Z. Liu, M. del Rosario, X. Liang, L. Zhang, and Z. Ding, "Spherical normalization for learned compressive feedback in massive MIMO CSI acquisition," in *2020 IEEE International Conference on Communications Workshops (ICC Workshops)*, 2020, pp. 1–6.
- [29] Z. Lu, X. Zhang, H. He, J. Wang, and J. Song, "Binarized aggregated network with quantization: Flexible deep learning deployment for CSI feedback in massive MIMO system," *IEEE Trans. Wireless Commun.*, pp. 1–1, 2022.
- [30] J. Guo, L. Wang, F. Li, and J. Xue, "CSI feedback with model-driven deep learning of massive MIMO systems," *IEEE Commun. Lett.*, pp. 1–1, 2021.
- [31] M. Soltani, V. Pourahmadi, A. Mirzaei, and H. Sheikhzadeh, "Deep learning-based channel estimation," *IEEE Commun. Lett.*, vol. 23, no. 4, pp. 652–655, 2019.
- [32] W. Utschick, V. Rizzello, M. Joham, Z. Ma, and L. Piazzini, "Learning the CSI recovery in FDD systems," *IEEE Trans. Wireless Commun.*, pp. 1–1, 2022.
- [33] P. Liang, J. Fan, W. Shen, Z. Qin, and G. Y. Li, "Deep learning and compressive sensing-based CSI feedback in FDD massive MIMO systems," *IEEE Trans. Veh. Technol.*, vol. 69, no. 8, pp. 9217–9222, 2020.
- [34] N. Turan, M. Koller, S. Bazzi, W. Xu, and W. Utschick, "Unsupervised learning of adaptive codebooks for deep feedback encoding in FDD systems," in *2021 55th Asilomar Conference on Signals, Systems, and Computers*, 2021, pp. 1464–1469.
- [35] M. Chen, J. Guo, C.-K. Wen, S. Jin, G. Y. Li, and A. Yang, "Deep learning-based implicit CSI feedback in massive mimo," *IEEE Trans. Commun.*, vol. 70, no. 2, pp. 935–950, 2022.
- [36] F. Sohrabi, K. M. Attiah, and W. Yu, "Deep learning for distributed channel feedback and multiuser precoding in FDD massive MIMO," *IEEE Trans. Wireless Commun.*, vol. 20, no. 7, pp. 4044–4057, 2021.
- [37] J. Guo, C.-K. Wen, and S. Jin, "Deep learning-based CSI feedback for beamforming in single- and multi-cell massive MIMO systems," *IEEE J. Sel. Areas Commun.*, vol. 39, no. 7, pp. 1872–1884, 2021.
- [38] V. Rizzello, N. Turan, M. Joham, and W. Utschick, "Two-sample tests for validating the UL-DL conjecture in FDD systems," in *2021 17th International Symposium on Wireless Communication Systems (ISWCS)*, 2021, pp. 1–6.
- [39] V. Rizzello, M. Nerini, M. Joham, B. Clerckx, and W. Utschick, "Learning representations for CSI adaptive quantization and feedback," *arXiv preprint arXiv:2207.06924*, 2022.
- [40] J. Zeng, J. Sun, G. Gui, B. Adebisi, T. Ohtsuki, H. Gacanin, and H. Sari, "Downlink CSI feedback algorithm with deep transfer learning for FDD massive MIMO systems," *IEEE Trans. Cogn. Commun. Netw.*, vol. 7, no. 4, pp. 1253–1265, 2021.
- [41] C. M. Bishop, *Pattern Recognition and Machine Learning*. Springer Verlag, Aug. 2006.
- [42] B. Clerckx, G. Kim, J. Choi, and S. Kim, "Allocation of feedback bits among users in broadcast MIMO channels," in *IEEE GLOBECOM 2008 - 2008 IEEE Global Telecommunications Conference*, 2008, pp. 1–5.
- [43] D. Tse and P. Viswanath, *Fundamentals of wireless communication*. Cambridge university press, 2005.
- [44] O. Bachem, M. Lucic, S. H. Hassani, and A. Krause, "Approximate k-means++ in sublinear time," in *Thirtieth AAAI conference on artificial intelligence*, 2016.
- [45] S. Jaeckel, L. Raschkowski, K. Börner, and L. Thiele, "QuADriGa: A 3-D multi-cell channel model with time evolution for enabling virtual field

- trials," *IEEE Trans. Antennas Propag.*, vol. 62, no. 6, pp. 3242–3256, 2014.
- [46] T. M. Cover, *Elements of information theory*. John Wiley & Sons, 1999.